processes

MDPI

Article

Experimental Investigation of Spherical Particles Settling in Annulus Filled with Rising-Bubble-Containing Newtonian Fluids

Silin Jing [1], Xianzhi Song [1], Mengmeng Zhou [1,*], Zhengming Xu [2], Zhaopeng Zhu [1] and Lei Wang [3]

[1] National Key Laboratory of Petroleum Resources and Engineering, China University of Petroleum, Beijing 102249, China; jingslcupb@163.com (S.J.); songxz@cup.edu.cn (X.S.); zhuzp@cup.edu.cn (Z.Z.)
[2] School of Energy Resources, China University of Geosciences, Beijing 100083, China; xuzm@cugb.edu.cn
[3] Sinopec Research Institute of Petroleum Engineering Co., Ltd., Beijing 102206, China; wanglei8.sripe@sinopec.com
* Correspondence: zhoumm@cup.edu.cn

Abstract: During the drilling of ultra-deep wells, gas kick often occurs, influenced by the complex void pressure profile. The accurate description of particle settling behavior in the gas–liquid mixture is of great significance to effectively deal with gas kicks and ensure drilling safety. In this study, the gas–liquid two-phase annulus flow with different gas volume fractions is created through the transparent annular pipe, constant pressure air pump, and gas flowmeter. High-speed photography is used to record and analyze the sedimentation of particles in gas–liquid mixtures. This study is based on 288 tests. The main parameters in this experiment include the particle Reynolds number, the gas fraction, and liquid viscosity. The effects of wall and gas fraction on the drag coefficient were analyzed. The correlation of particle terminal settling velocity was established. The results obtained show a correlation with average absolute errors (AAE) of 10.7%. This study reveals the settling characteristics of particles in the annular gas–liquid mixed flow, provides an accurate terminal settling velocity prediction explicit formula, and provides guidance for the calculation of bottom hole pressure under the condition of gas kick.

Keywords: particle terminal settling velocity; gas–liquid two-phase; annulus; gas volume fractions; particle Reynolds number; liquid viscosity; the drag coefficient; explicit formula

Citation: Jing, S.; Song, X.; Zhou, M.; Xu, Z.; Zhu, Z.; Wang, L. Experimental Investigation of Spherical Particles Settling in Annulus Filled with Rising-Bubble-Containing Newtonian Fluids. *Processes* **2024**, *12*, 1474. https://doi.org/10.3390/pr12071474

Academic Editor: Haiping Zhu

Received: 23 June 2024
Revised: 9 July 2024
Accepted: 12 July 2024
Published: 14 July 2024

1. Introduction

In the field of the oil and gas industry, the development of oil and gas inevitably depends on the establishment of oil and gas wells, which involve the solid–liquid two-phase wellbore flow process during drilling [1,2], completion [3,4], and production [5]. The scientific study of these processes involves the settling velocity of solid particles. Accurate prediction of particle settling velocity will have an important impact on wellbore pressure calculation and cuttings removal process implementation. Based on the above engineering situation, a large number of particle settlement studies have been carried out by predecessors, which involve variables such as fluid properties, particle properties, and wellbore size. However, under the condition of gas invasion, the particle settlement environment is the annular condition composed of wellbore and drill pipe, accompanied by bubble rise, and the particle settlement characteristics under this condition are very different from previous studies. Therefore, the particle settling velocity of ultra-deep gas wells under gas invasion conditions remains to be further studied. The settling law of spherical particles in an annular wellbore under the gas–liquid two-phase condition is studied in this paper, which is of great significance for the safe well construction of oil and gas wells.

Since the Stokes formula, a lot of studies have been carried out to study the free-settling properties of particles. Okorie et al. [6] summarized the research on the settling rate of

drilling cuttings in drilling fluid and conducted a review from the aspects of experiment, numerical simulation, and artificial intelligence. Among them, 91 experimental studies were conducted, and related studies were conducted on the properties of different particles and fluids. Sze-Foo et al. [7] studied the settling velocity of irregular particles. C. Lareo et al. [8] studied the settling velocity of different particle densities. VASSILIOS et al. [9] studied the free sedimentation of solid particles in Newtonian and non-Newtonian fluids and proposed a prediction formula for particle sedimentation velocity. For spherical particles, Cheng et al. [10], based on the experimental data collected by predecessors, proposed prediction formulas for the terminal settling velocity and drag coefficient of particles with a Reynolds number up to 2×10^5 and compared the accuracy with eight prediction formulas proposed by predecessors. Sahil et al. [11] carried out an experimental study on the settling of spherical particles in an unbounded and restricted surfactant shear-thinning viscoelastic fluid. L.H. Childs et al. [12], considering that the dynamic sedimentation of fluid is affected by the dynamic change of fluid properties, proposed the dynamic sedimentation law of particles in shear-dilution fluid. J. Faitli [13] developed the settling characteristics in two-phase media and proposed a new experimental device to measure the settling velocity of steel balls in a fine-particle solid–water mixture. Previous studies on particle deposition have been carried out in various special cases. In summary, it can be found that the characteristics of particles settling in different working conditions need experimental rules to carry out mechanical research. In addition, different settling geometry environments also have important effects on particle settling. Chhabra [14,15] carried out a study on the influence of wall surfaces on the free-settling velocity of non-spherical particles in viscous media. Given the wall effect, Arsenijevic [16], Shuai [17], and Song [18] carried out experimental studies on particle sedimentation of different fluids and particle properties and put forward corresponding prediction models. Zhu et al. [19] also proposed a unified formula for particle settling velocity by comparing the particle settling properties under geometric space conditions such as cylinder, annulus, and fracture. In summary, it is found that the wall effect is an important factor affecting particle settling, which must be considered under practical engineering conditions. The introduction of the wall effect has a positive impact on the prediction accuracy of particle settling velocity. In addition, the study of particle settling velocity under bubble rising environment is still rarely reported. Jing [20] and Issoufou et al. [21] studied the particle settling behavior of spherical particles in cylinders in Newtonian and non-Newtonian fluids, respectively, and established prediction correlations from the perspective of mechanism and dimensionless methods, respectively. However, under the condition of oil drilling, the engineering environment is in the annulus, not in the cylinder, and the particle settling characteristics are different under the two environments. At present, there is still no study on the characteristics of particles settling in the gas–liquid phase under annular conditions.

In this study, the wellbore environment with bubble rise was simulated under annular conditions. Under different gas volume fractions, particle sizes, particle densities, and fluid viscosities, 288 sets of particle settling experiments were carried out. High-speed photography was used to capture particle settling behavior and calculate the terminal velocity of particle settling. The effect of the wall and rising bubble on the drag coefficient of the particles is analyzed, and a dimensionless correlation for predicting the terminal velocity of the particles is established.

2. Materials and Methods

2.1. Experimental Setup

As shown in Figure 1a, the particle settling simulation and measurement system includes a transparent annulus wellbore, an air compressor, and a high-speed camera system. The outer diameter of the transparent annulus wellbore is 165 mm, the outer diameter of the inner pipe is 140 mm, and the height is 1.60 m. The height of the annulus wellbore is sufficient for the particles to reach the terminal settling velocity and the bubbles to rise steadily. As shown in Figure 1b, a bubble-generating ring is placed at the bottom

of the transparent annulus wellbore, which can uniformly generate bubbles and simulate the environment of bubbles rising. The outlet of the air compressor is equipped with a control valve and a gas flowmeter, which can realize the stable control and measurement of the gas flow. The gas flowmeter is connected to the bubble generation ring through a thin tube to control and measure the gas flow rate. In addition, a high-speed camera system is installed on the outside of the wellbore, which includes a high-speed camera and accompanying software Phantom Camera Control (PCC) V310 to calculate the terminal settling velocity of spherical particles. The processing of the terminal settling velocity by PCC V310 is divided into three parts: setting and debugging, shooting and storing, and calibrating the speed. In setting and debugging, the parameters such as shooting rate, exposure time, and resolution are mainly adjusted under different particle and gas–liquid environments to find the most reasonable range. In the process of shooting, the influence of gas volume fraction should be considered, camera position and lens focus should be set, the image should be edited, and the experiment should be divided into steps to achieve the goal of the least memory consumption and the most efficient analysis. The software calibration mainly uses the calculation of distance, focal length, and image reference scale to calculate the distance between two points of the image, combined with the shooting time of two points to calculate the terminal settling velocity.

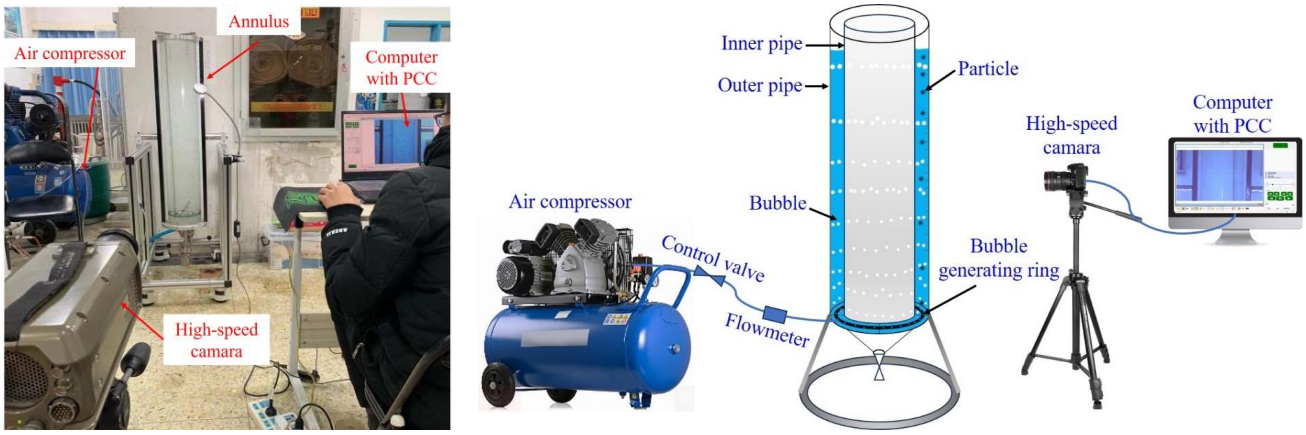

Figure 1. (**a**) The actual photo of the experimental setup; (**b**) detailed schematic diagram of the experimental setup.

2.2. Experimental Materials and Fluids

Three kinds of density particles were used in the particle settling experiment, namely aluminum alloy particles (2710 kg/m^3), zirconia particles (5826 kg/m^3), and ferroalloy particles (7860 kg/m^3), and the diameter of the particles ranged from 3 to 10 mm. A total of 4 fluids were used in the experiment, namely water and glycerol with different mass concentrations (10 wt% glycerol, 20 wt% glycerol, 30 wt% glycerol). The ZNN-D6B Model 6-speed rotational viscometer was used to determine rheological characteristics of the fluids. The density and viscosity of the measured fluids are shown in Table 1.

Table 1. Test matrix.

Particle Density (kg/m^3)	Particle Size (mm)	Fluid Type	Fluid Density (kg/m^3)	Fluid Viscosity (Pa.s)
Al: 2710 ZrO_2: 5826 Fe:7860	3/4/5/6/8/10	Water	998.200	0.0010
		10 wt% glycerol	1009.568	0.0015
		20 wt% glycerol	1035.027	0.0018
		30 wt% glycerol	1070.613	0.0030

2.3. Experimental Method

To ensure the accuracy of the measured particle's terminal settling velocity in the annulus containing rising bubbles, the experimental procedure is as follows:

(1) Configuration solution: The electronic scale and stirrers are equipped with 10 wt% glycerol, 20 wt% glycerol, and 30 wt% glycerol mass concentration Newtonian fluid for reserve. The viscosity of the experimental fluid is measured with a 6-speed rotating viscometer before the experiment (it must be before bubble disturbance to avoid the influence of bubble disturbance on the fluid's rheology). Then, the transparent annulus wellbore is filled with the experimental fluid, and the fluid experiment sequence is pure water, 10 wt% glycerol, 20 wt% glycerol, and 30 wt% glycerol.

(2) Adjust the gas flow: Adjust the gas flow to the preset value and wait for it to stabilize to ensure that the bubbles in the shooting area are more uniform. Adjust the shooting area of the high-speed camera system, the exposure, and the number of shooting frames of the photography software (the number of shooting frames is 200 frames/SEC), the movement of the spherical particles in the shooting area is clear to ensure that the particles in the shooting area reach the terminal settling speed, and the high-speed camera system must be maintained level.

(3) Throwing particles: Open the camera mode of high-speed photography, put the spherical particles below the liquid level to ensure that the initial speed of the particles is zero, and repeat throwing the same particles 5 times. The settling process of the spherical particles is saved as a photographic file, and the terminal settling velocity of the spherical particles is calculated by the PCC V310 system and saved. As shown in Figure 2, the particle settling process can be analyzed by the PCC V310 system (calibration distance, frame rate, calculation of settling velocity).

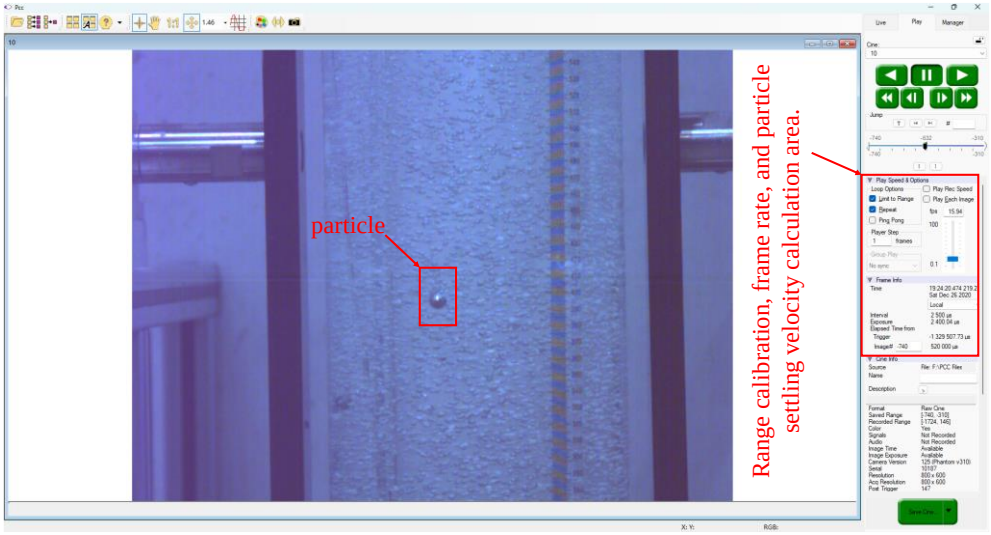

Figure 2. The sedimentation process of 10 mm aluminum alloy particles in water with a gas flow rate of 5 L/min was captured by the PPC system.

(4) Repeat steps: Adjust the different gas flow, particle type, and fluid type, repeat the above steps.

2.4. Determination of Gas Volume Fraction

In this experiment, the settling of particles under several experimental conditions is completed under the condition of gas entry. The fluid in the wellbore rises as the gas is pumped in, which changes the density of the fluid. The gas content under different glycerol mass concentrations and different ventilation are shown in Table 2. This paper sets

a formula to describe the gas content after gas injection, which involves the variation of the liquid height level. The formula is as follows:

$$G_C = \frac{H_A - H_B}{H_A}, \quad (1)$$

where H_B is the liquid level height before the gas injection, m; H_A is the liquid level height after gas injection, m; and G_C is the gas content after the gas injection, dimensionless.

Table 2. The gas content in gas–liquid two-phases in different fluids.

Mass Concentration	The Gas Content of Gas–Liquid Two-Phase			
	0.0 L/min	5.0 L/min	10.0 L/min	15.0 L/min
0.0% Glycerol	0.0000	0.03430	0.06543	0.09546
10.0% Glycerol	0.0000	0.04034	0.06585	0.10112
20.0% Glycerol	0.0000	0.03760	0.07371	0.09742
30.0% Glycerol	0.0000	0.03066	0.05424	0.07621

3. Experimental Results and Analysis

A total of 288 groups of particle settling experiments were carried out, each group repeated 5 times, and a total of 1440 times particles were dropped. The terminal settling velocity is the average value of five settling experiments in each group, and the standard error of each group is calculated. The average standard error of 288 groups is 0.0249. It indicates that the experimental results are reproducible to some extent.

3.1. Validation of Particle Terminal Settling Velocity

Since scholars have carried out a large number of studies on particle free settling, experiments without gas are used to verify particle terminal settling velocity. In Figure 3, 72 groups of particle terminal settling velocity without gas in this experiment are compared with that of particle free terminal settling velocity, and the results show that the relative error between small particle terminal settling velocity and particle free terminal settling velocity is lower. It shows that the drag coefficient of large particles increases due to the influence of the wall effect [22] in the annulus. The comparison results of particle terminal settling velocity are shown in Figure 3.

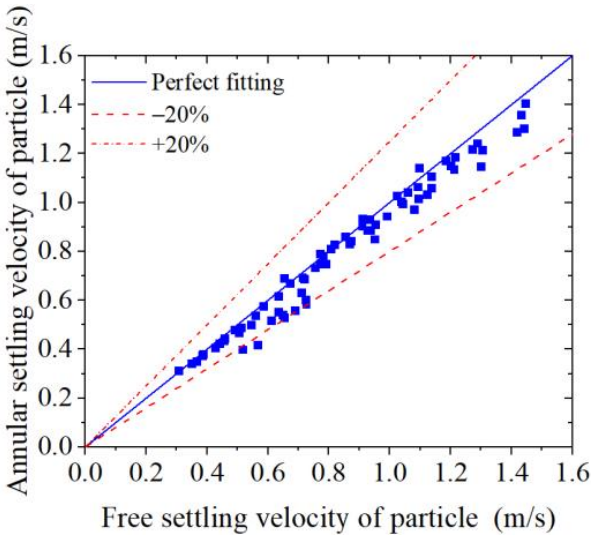

Figure 3. The particle settling velocity without bubbles in the annulus is compared with the particle free settling velocity.

In the calculation model of particle free settling, the Cheng model [10] is widely used to verify the accuracy of particle free settling data. The formula for calculating the drag coefficient of particles is as follows:

$$\begin{cases} C_D = \frac{24}{\mathrm{Re}}(1 - 0.27\mathrm{Re})^{0.43} + 0.47\left[1 - \exp(-0.04\mathrm{Re}^{0.38})\right] \\ \mathrm{Re} = \frac{\rho d v}{\mu} \end{cases}, \quad (2)$$

where C_D is the drag coefficient of particles, dimensionless; Re is the particle Reynolds number, dimensionless; ρ is the density of liquid, kg/m^3; d is the diameter of particle, m; v is the terminal settling velocity of particle, m/s; and μ is the viscosity of liquid, mPa·s.

In addition, the actual drag coefficient is calculated according to Formula (3) and, compared with the drag coefficient calculated by the Cheng model, it is found that the relative error of particles with small particle sizes of 3 and 4 mm is only 3%. As shown in Figure 4, the experimental data are those of particles with particle sizes of 3 and 4 mm that settle in an environment without gas, and the Reynolds number ranges from 332.40 to 3702.44. Although the particle size is much smaller than the annulus size, the experimental results are also slightly larger than those calculated by the Cheng model. The actual drag force is slightly greater than the drag force of free settling, indicating that the annular drag force is affected by the wall effect, and the drag coefficient of the particles increases to a certain extent, which proves that the experimental data are of practical significance.

$$C_D = \frac{4(\rho_s - \rho)dg}{3\rho v^2}, \quad (3)$$

where ρ_s is the density of a particle, kg/m^3; g is gravitational acceleration, m/s^2.

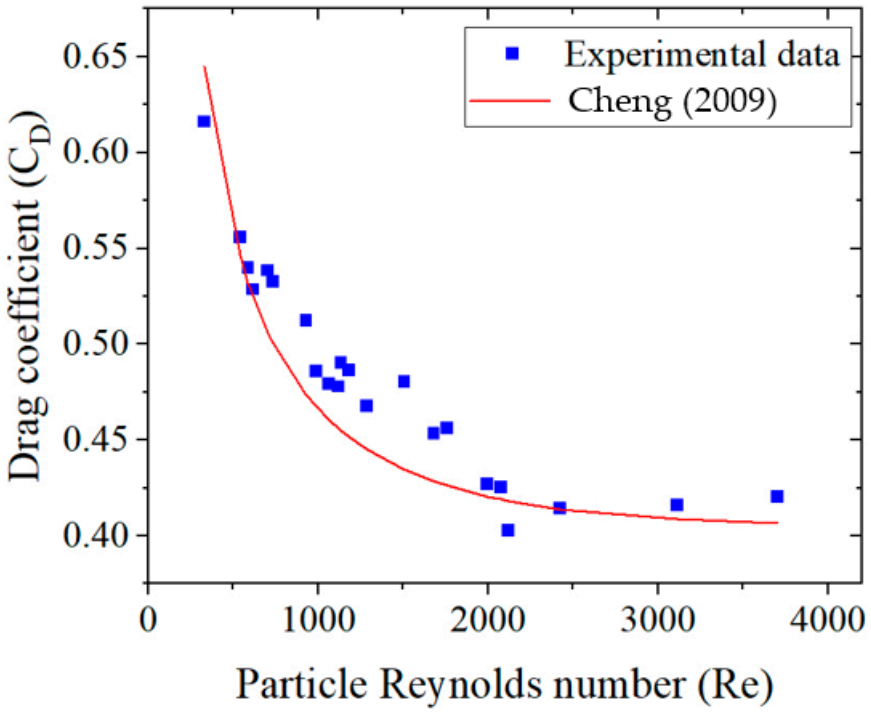

Figure 4. The drag coefficient vs. particle Reynolds number of sphere particles without bubbles in the annulus [10].

3.2. The Influence of Vertical Annular Wall Effect on Drag Coefficient

As particles are thrown into the same annulus (D_O = 165 mm, D_I = 140 mm), the spherical particle size increases and the dimensionless diameter increases, defined as follows:

$$d^* = 2d/(D_O - D_I), \tag{4}$$

where d^* is the dimensionless diameter, dimensionless; D_O is the outer diameter of the annulus, m; and D_I is the inner diameter of the annulus, m.

As shown in Figure 5, the variation law of particle in annulus drag coefficient with Reynolds number (332.40–12,990.575) without gas injection is calculated experimentally. The particle drag coefficients with dimensionless diameters of 0.24, 0.40, and 0.64 were calculated. The dimensionless particle size corresponds to the particle sizes of 3, 5, and 8 mm, respectively. The results show that the C_D increases with the increase of the d^* compared with the C_D of the particle free terminal settling velocity, indicating that the drag coefficient caused by the wall effect increases.

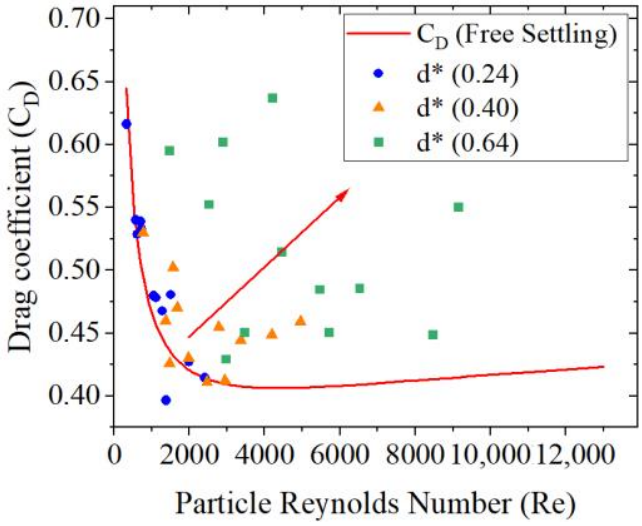

Figure 5. Drag coefficient vs. particle Reynolds number without bubbles in the annulus.

3.3. The Influence of Rising Bubbles on the Drag Coefficient

As shown in Figure 6a, the force diagram of particles settling freely in the annulus with bubbles rising is shown. The spherical particles rising in the annulus with bubbles are mainly affected by their own gravity, buoyancy, flow resistance, wall resistance, and the lifting force of bubbles. Figure 6b shows the formula of force on particles. F_{WO} is the net weight force, that is, the gravity of the particle minus the buoyancy force. F_f is the resistance of the fluid to the particle when it settles, and C_{DF} is the drag coefficient of the fluid. F_b is the lifting force of the bubble on the particle, and C_{Db} is the lifting force coefficient. F_{dw} is the wall resistance to particle settling, and C_{Dw} is the wall resistance coefficient. In this paper, by analyzing the force relationship of particles in a fluid with rising bubbles, the key factors affecting the force of particles and their final settling velocity are obtained, and the basis is provided for the analysis of the difference between the drag data of particles in a fluid with bubbles in the annulus and that of free settling particles.

As shown in Figure 7, terminal settling velocity data of large particles with a dimensionless diameter of 0.64 were selected to calculate the drag coefficient. The experiment found that the drag coefficient of particles without gas injection in the annulus was larger than that of particles free settling, and after gas injection, the drag coefficient of particles was smaller than that of particles free settling. According to the analysis, when gas is injected, the density of the gas–liquid mixture decreases and the particle settling velocity increases. According to Formula (3), the drag coefficient should be the drag coefficient of free settling in the red line. However, due to the drag force of the bubble, the drag

coefficient is higher or lower than that of free settling, but it is lower than that of particle settling without gas in the annulus. This phenomenon shows that the effect of the drag force of the bubble on the particles is related to the collision between the bubble and the particles, which is somewhat random. However, under the same annulus condition, the drag coefficient of the particles will certainly be reduced by gas injection, but whether the drag coefficient is lower than that of free settling needs to be considered.

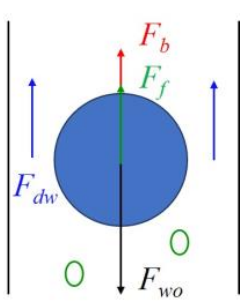

(**a**)

$$\begin{cases} F_{wo} = \dfrac{\pi}{6} d^3(\rho_s - \rho)g \\ F_f = \dfrac{\pi}{8} C_{Df} v^2 \rho d^2 \\ F_b = \dfrac{\pi}{8} C_{Db} v^2 \rho d^2 \\ F_{dw} = \dfrac{\pi}{8} C_{Dw} v^2 \rho d^{*2} \end{cases}$$

(**b**)

Figure 6. (**a**) The force diagram of particles settling freely in the annulus with bubbles rising; (**b**) force mechanics formula of particles in the annulus with bubbles rising.

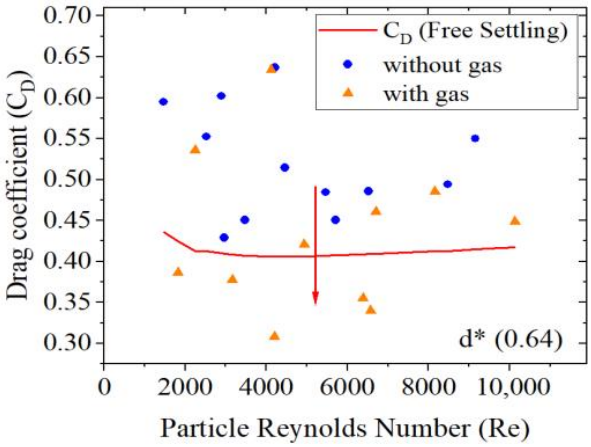

Figure 7. Drag coefficient vs. particle Reynolds number of sphere particle with bubbles in the annulus.

4. Correlation of the Particle Terminal Settling Velocity

Dimension analysis is a powerful means and method to analyze and solve problems, which can describe the relationship between different parameters well and has been applied in many fields. Next, a correlation of the terminal settling velocity of spherical particles in the annular air–liquid phase is established by the dimensional analysis method.

The particle settling velocity is mainly affected by the drag force on the particles. According to the analysis in Figure 5, besides the main factors concerned by previous studies, the gas content in the experiment is an important factor concern in this paper. The main factors affecting the terminal settling velocity are particle density ρ_s, fluid viscosity μ, particle diameter d, fluid density ρ, gravitational acceleration g, and gas content G_C.

$$f(v,\ \rho_s,\ \mu,\ d,\ \rho,\ g, G_C) = 0, \tag{5}$$

According to the theorem of π, four dimensionless terms are selected, which have the following functional relations:

$$F(\pi_1,\ \pi_2,\ \pi_3,\ \pi_4) = 0, \tag{6}$$

According to the theorem of dimensional homogeneity, four concrete expressions of dimensionless π terms can be obtained. The expression for the 4 π is shown in Table 3:

Table 3. Dimensionless terms of fitting results.

Dimensionless Terms	Fitting Results
π_1	$vd^{-\frac{1}{2}}g^{-\frac{1}{2}}$
π_2	$\rho_s\rho^{-1}$
π_3	$\rho^{-1}d^{-\frac{3}{2}}g^{-\frac{1}{2}}$
π_4	G_C

When dealing with experimental or numerical results, it is usually possible to express the results as a power relationship, namely:

$$\begin{cases} \pi_1 = \varphi(\pi_2, \pi_3, \pi_4) \\ \pi_1 = k \cdot {\pi_2}^a \cdot {\pi_3}^b \cdot {\pi_4}^c \end{cases}, \tag{7}$$

Take the natural logarithm of both sides of Formula (7), as follows:

$$\ln \pi_1 = \ln k + a \ln \pi_2 + b \ln \pi_3 + c \ln \pi_4, \tag{8}$$

Using the experimental data, multivariate linear fitting was performed, and the following results were obtained; the fitting correlation coefficient R^2 was 0.80429, and the fitting effect met the accuracy required by the project:

$$\begin{cases} \ln k = 0.18219 \\ a = 0.65972 \\ b = 0.03676 \\ c = -0.06708 \end{cases}, \tag{9}$$

The fitting results were processed with Formula (7), and the fitting formula is shown below. Formula (10) is the prediction correlation of the terminal settling velocity of spherical particles under the annular air–liquid two-phase condition:

$$v = e^{0.18219} \cdot d^{\frac{1}{2}} \cdot g^{\frac{1}{2}} \cdot \left(\frac{\rho_s}{\rho}\right)^{0.65972} \cdot \left(\frac{\mu}{\rho d^{\frac{3}{2}} g^{\frac{1}{2}}}\right)^{0.03676} \cdot {G_C}^{-0.06708} \tag{10}$$

Figure 8 is the comparison between the calculated value of the terminal settling velocity prediction correlation and the terminal settling velocity measured by experiments. The three straight lines in the figure are, respectively, +20% error lines, 0 error lines, and −20% error lines from top to bottom. As can be seen from the figure, most of the data points are within the 20% error line, and the average relative error between the calculated experimental value and the predicted value of the correlation is 10.70%. The analysis shows that there are two main reasons leading to the error: one is the influence of the measuring environment. When the particle terminal settling velocity is small, the particle settling process is easily affected by the surrounding environment, and the data error is relatively large. The second is the error generated in the process of data fitting.

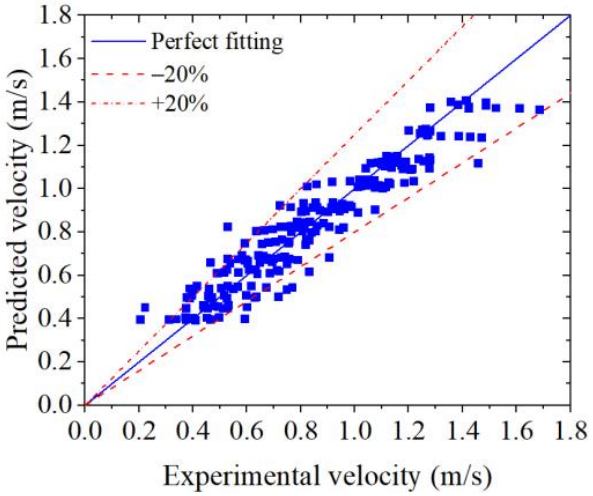

Figure 8. Comparison of predicted velocity with experimental value.

5. Conclusions

The particle settling experiment has been extended from the free settling of the wellbore to the annulus particle settling, and this study extends to the annulus particle settling considered by the bubbles.

In this study, an experimental device is proposed to simulate the atmosphere of the annular bubble rising. The terminal settling velocity of particles with different gas volume fractions, fluid viscosities, and particle properties in this environment is calculated by a high-speed photographic system.

The results show that the annular particle settling is affected by the wall effect, and the particle terminal settling velocity slows down, but the existence of bubbles weakens the effect of the wall effect. It is found that the impact of bubble lifting force is much smaller than the effect of fluid density reduction by bubble.

Based on the randomness of bubble rise, an explicit expression for displaying the terminal velocity of particle settling is established by dimensional analysis. The fitting correlation coefficient R^2 was 0.80429, and the average relative error between the predicted value and the experimental value was 10.70%.

In the future, the influence of high temperature and high pressure on gas and fluid can be considered to provide a theoretical basis for the calculation of three-phase flow in ultra-deep wells.

Author Contributions: Conceptualization, X.S.; Formal analysis, S.J.; Investigation, S.J., M.Z. and Z.X.; Methodology, S.J., Z.Z. and Z.X.; Writing—original draft, S.J.; Writing—review and editing, M.Z., Z.X., L.W. and Z.Z. All authors have read and agreed to the published version of the manuscript.

Funding: The authors express their appreciation to the National Science Foundation of China (No. 52274019, No. 52125401, Grant No. 52192624), the Science Foundation of China University of Petroleum, Beijing (No. 2462022QNXZ004), and the National Key Laboratory of Petroleum Resources and Engineering (No. PRE/indep-3-2306) for their financial support.

Data Availability Statement: The original contributions presented in the study are included in the article, further inquiries can be directed to the corresponding author.

Acknowledgments: The authors would like to thank the anonymous reviewers for their valuable comments.

Conflicts of Interest: Author Lei Wang was employed by the company Sinopec Research Institute of Petroleum Engineering Co., Ltd. The remaining authors declare that the research was conducted in the absence of any commercial or financial relationships that could be construed as a potential conflict of interest.

References

1. Jing, S.; Song, X.; Zhou, M.; Xu, Z.; Sun, Y.; Xiao, H.; Abou-Kassem, A.; Kuru, E. Experimental investigation of the annular cross-sectional distribution of cuttings bed with drillpipe rotation in horizontal wells. *Powder Technol.* **2024**, *436*, 119520. [CrossRef]
2. Tomren, P.H.; Lyoho, A.W.; Azar, J.J. Experimental Study of Cuttings Transport in Directional Wells. *SPE Drill. Eng.* **1986**, *1*, 43–56. [CrossRef]
3. Isah, A.; Hiba, M.; Al-Azani, K.; Aljawad, M.S.; Mahmoud, M. A comprehensive review of proppant transport in fractured reservoirs: Experimental, numerical, and field aspects. *J. Nat. Gas Sci. Eng.* **2021**, *88*, 103832. [CrossRef]
4. Ozbayoglu, M.E.; Saasen, A.; Sorgun, M.; Svanes, K. Effect of pipe rotation on hole cleaning for water-based drilling fluids in horizontal and deviated wells. In Proceedings of the IADC/SPE Asia Pacific Drilling Technology Conference and Exhibition, Jakarta, Indonesia, 25–27 August 2008.
5. Khaksar, A. Use of Advanced Geomechanical Analysis to Define Practical Cut-Offs for Sand Control Decisions. In Proceedings of the International Petroleum Technology Conference, Dhahran, Saudi Arabia, 12 February 2024.
6. Agwu, O.E.; Akpabio, J.U.; Alabi, S.B.; Dosunmu, A. Settling velocity of drill cuttings in drilling fluids: A review of experimental, numerical simulations and artificial intelligence studies. *Powder Technol.* **2018**, *339*, 728–746. [CrossRef]
7. Chien, S.-F. Settling velocity of irregularly shaped particles. *SPE Drill. Complet.* **1994**, *9*, 281–289. [CrossRef]
8. Lareo, C.; Branch, C.A.; Fryer, P.J. Particle velocity profiles for solid-liquid food flows in vertical pipes part I. Single particles. *Powder Technol.* **1997**, *93*, 23–34. [CrossRef]
9. Kelessidis, V.C. Terminal velocity of solid spheres falling in Newtonian and non-Newtonian liquids. *Tech. Chron. Sci. J. TCG* **2003**, *5*, 43–54.
10. Cheng, N.-S. Comparison of formulas for drag coefficient and settling velocity of spherical particles. *Powder Technol.* **2009**, *189*, 395–398. [CrossRef]
11. Malhotra, S.; Sharma, M.M. Settling of spherical particles in unbounded and confined surfactant-based shear thinning viscoelastic fluids: An experimental study. *Chem. Eng. Sci.* **2012**, *84*, 646–655. [CrossRef]
12. Childs, L.; Hogg, A.; Pritchard, D. Dynamic settling of particles in shear flows of shear-thinning fluids. *J. Non-Newton. Fluid Mech.* **2016**, *238*, 158–169. [CrossRef]
13. Faitli, J. Continuity theory and settling model for spheres falling in non-Newtonian one- and two-phase media. *Int. J. Miner. Process.* **2017**, *169*, 16–26. [CrossRef]
14. Chhabra, R. Wall effects on free-settling velocity of non-spherical particles in viscous media in cylindrical tubes. *Powder Technol.* **1995**, *85*, 83–90. [CrossRef]
15. Chhabra, R. Wall effects on terminal velocity of non-spherical particles in non-Newtonian polymer solutions. *Powder Technol.* **1996**, *88*, 39–44. [CrossRef]
16. Arsenijević, Z.L.; Grbavčić, Ž.; Garić-Grulović, R.; Bošković-Vragolović, N. Wall effects on the velocities of a single sphere settling in a stagnant and counter-current fluid and rising in a co-current fluid. *Powder Technol.* **2010**, *203*, 237–242. [CrossRef]
17. Tian, S. Wall effects for spherical particle in confined shear-thickening fluids. *J. Non-Newton. Fluid Mech.* **2018**, *257*, 13–21. [CrossRef]
18. Song, X.; Zhu, Z.; Xu, Z.; Li, G.; Faustino, M.A.; Chen, C.; Jiang, T.; Xie, X. Experimental study on the wall factor for spherical particles settling in parallel plates filled with power-law fluids. *J. Pet. Sci. Eng.* **2019**, *179*, 941–947. [CrossRef]
19. Zhu, Z.; Zhou, M.; Yu, B.; Song, X.; Li, G.; Zhu, S.; Xu, Z.; Yao, X.; Liu, Z. A unified equation of settling velocity for particles settling in cylinder, annulus and fracture. *J. Pet. Sci. Eng.* **2022**, *213*, 110446. [CrossRef]
20. Jing, S.; Song, X.; Zhu, Z.; Yu, B.; Duan, S. Settling Behavior of Particles in Bubble Containing Newtonian Fluids: Experimental Study and Model Development. In Proceedings of the ASME 2021 40th International Conference on Ocean, Offshore and Arctic Engineering, Virtual, 21–30 June 2021.
21. Issoufou, M.K.; Song, X.; Zhu, Z.; Xu, Z.; Yu, B.; Jing, S.; Duan, S. Predicting cuttings settling velocity in drilling muds and in rising-bubbles-containing muds. *J. Pet. Sci. Eng.* **2021**, *204*, 108766. [CrossRef]
22. Chhabra, R.; Uhlherr, P. Wall effect for high Reynolds number motion of spheres in shear thinning fluids. *Chem. Eng. Commun.* **1980**, *5*, 115–124. [CrossRef]